IC/89/36
INTERNAL REPORT
(Limited Distribution)

International Atomic Energy Agency
and
United Nations Educational Scientific and Cultural Organization
INTERNATIONAL CENTRE FOR THEORETICAL PHYSICS

UPPER IONOSPHERE AND MAGNETOSPHERIC–IONOSPHERIC COUPLING*

J.R. Manzano**
International Centre for Theoretical Physics, Trieste, Italy.

MIRAMARE – TRIESTE
February 1989

* To be published in the Proceedings of the ICTP College on Theoretical and Experimental Radiopropagation Physics, 6–24 February 1989, Trieste, Italy.

** Permanent address: Faculty of Exact Sciences and Technology, Institute of Physics, University of Tucuman, Tucuman, Argentina.

I. IONOSPHERIC PHYSICS

I.1 Introduction

The ionosphere is usually defined as the region of the Earth's atmosphere which contains enough electrons and ions as to affect the radio waves propagation. With this definition the lower border could go down to 50 km. The upper border is undefined, but considered "by decree" about 1000 km.

The ionosphere existence has been postulated by Heaviside and Kennelly in 1902, to explain propagation through long distances. The first direct observation of downwards reflected radio waves was achieved by Appleton and Barnett 23 years later. The technics, basis of the actual ionosonde, was developed by Breit and Tuve shortly afterwards.

A vertically directed pulse is reflected at the level at which the radio frequency equals the plasma oscillation frequency

$$f_N' = \frac{\pi}{2}\left(\frac{Ne^2}{m\varepsilon_0}\right)^{1/2}$$

where N = electron concentration; e and m = electron charge and mass;
ε_0 = free space electric permittivity

$$N(\text{elect}/m^3) = (1/e^2)4\pi^2\varepsilon_0 m f_N^2 = 1.24 \times 10^{10} f_N^2 \quad \text{with } f_N \quad \text{in } Mc/s\,.$$

Historically, Appleton first discovered the E-region. The more or less accepted convention refers to ionosphere below 90 km as D-region; E-region lies between 90 and 160 km; F-region above 160 km. Any structure within a region is usually denoted by adding a subindex 1,2, ... so that the F_1 region lies below the F_2 peak. A rough idea is given by Fig. 1 [1].

I.2 Photoionization

A fundamental process for creation of the ionosphere is the photoionization. The theory was developed by Chapman [2a,b]. He derived a formula for the ionization production rate q as a function of height h, and sun's zenith angle, χ, introducing the following simplifying assumptions:

a) there is no waste of neutral atmosphere. The fraction of ionized gas is extremely small;

b) there is only a single absorbing gas, with concentration $n(h)$;

c) the neutral gas is subject to ideal gases law, $p = n \cdot k \cdot T$;

d) the atmosphere is plane and horizontally stratified. Chapman extended the theory to a curved Earth;

e) the solar radiation is monochromatic, with a photon flux $I(h)$;

f) the scale height, $H = kT/mg$, is independent or linear changing with height;

g) the atmosphere is exponential. It means

$$p/p_0 = n/n_0 = \rho/\rho_0 = \exp(-(h - h_0)/H)$$

where p = pressure, n = concentration, ρ = mass density and p_0, n_0, ρ_0 are values at reference level h_0.

Calling σ to the cross section for radiation absorption, n to the ionising efficiency, and with the preceding assumptions, Chapman obtained the final expression

$$q = q_m \cdot \exp(1 - z - e^{-z}) \tag{1}$$

where

$$q_m = I_m \cdot \eta \cdot \sigma \cdot n_m;\ z \equiv \text{ reduced height } = (h - h_0)/H$$

with m characterising the value of the parameter at the height of maximum production. For sun overhead ($\chi = 0$), (1) becomes

$$q = q_{m_o} \exp(1 - y - \sec\chi e^{-y}) \tag{2}$$

where

$$q_{m_o} = q_m \cdot \sec\chi; \quad y = (h - h_{m_o})/H$$

For a linear variation of H, $\Gamma = dH/dh$ = constant, the final expression is

$$\begin{aligned} q &= q_m(\sec\chi)^{1+\Gamma} \exp((1+\Gamma)(1 - y - e^{-y}\sec\chi)) \\ &= q_{m_o} \exp((1+\Gamma)(1 - y - e^{-y}\sec\chi)) \end{aligned} \tag{3}$$

where

$$q_{m_o} = \frac{I_\infty \eta}{H_{m_o}}(1+\Gamma)e^{-(1+\Gamma)};\ q_m = \frac{I_\infty \eta}{H_m \sec\chi}(1+\Gamma)e^{-(1+\Gamma)}$$
$$H_m = H_{m_o}(\sec\chi)^\Gamma$$

Eq.(1) is represented in Fig. 2 [3]. It shows that

(i) $q(h, \chi)$ maintains its shape when χ changes,

(ii) the amplitude is affected by a factor $\cos\chi$,

(iii) the maximum shifts to y_m.

Eq.(3) shows a similar behaviour, but the amplitude is affected by a $(\cos\chi)^{1+\Gamma}$ factor. Analogue behaviour for y_m but curves are broader.

I.3 E–Region

The E–layer is considered a good approximation to the idealized Chapman layer, and into a into photochemical regime, although transport processes may produce significant perturbations.

I.3.1 Ionization Sources Solar radiation at wavelengths shorter than 3200 A (320 nm) is totally absorbed in Earth's upper atmosphere. Although UV region accounts for less than 2% of total irradiance, it is the principal source of energy in the upper atmosphere and controls the neutral and ion composition, temperature, and photochemistry in the stratosphere, mesosphere, and thermosphere. This aborption of UV is shown in Fig. 3 [4].

Soft X-rays, 10-150 A(1-15 nm), and EUV from 800-1800 A (80 - 180 nm), ionize the E-region, except the interval including the Ly alpha, which acts preferably at D–region. At E-region O_2 is the main absorber, forming O_2^+. X-rays would ionize all constituents forming N_2^+, O_2^+, and O^+. Due to subsequent reactions, NO^+ and O_2^+ are the most abundant.

I.3.2 Chemistry In E-region, negative ions are virtually absent. Produced by electron attachment, are rapidly destroyed by photodetachment in daylight and quite rapidly by ionic recombination. Dissociative recombination of electrons and molecular positive ions is the only important recombination process $\rightarrow X^+ + YZ \rightarrow XY^+ + Z$, recombining with electrons.

Ions behaviour strongly depends of sun's zenith angle. As can be seen in Figs.4 and 5 [5] NO^+ and O_2^+ are the most important ions.

The following table shows photochemical reactions possible in E and F regions

Photoionization	(rate, q)
$O + h\nu \rightarrow O^+ + e$	$(Q1)$
$N_2 + h\nu \rightarrow N_2^+ + e$	$(Q2)$
$O_2 + h\nu \rightarrow O_2^+ + e$	$(Q3)$

Transfer or interchange	(rate coefficient, γ)
$O^+ + N_2 \rightarrow NO^+ + N$	$(T1)$
$O^+ + O_2 \rightarrow O_2^+ + O$	$(T2)$
$N_2^+ + O \rightarrow NO^+ + N$	$(T3)$
$N_2^+ + O \rightarrow O^+ + N_2$	$(T4)$
$N_2^+ + O_2 \rightarrow O_2^+ + N_2$	$(T5)$
$O_2^+ + N_2 \rightarrow NO^+ + NO$	$(T6)$

Dissociative recombination	(rate coefficient, α)
$O_2^+ + e \rightarrow O^* + O^{**}$	$(R1)$
$NO^+ + e \rightarrow N^* + O^*$	$(R2)$
$N_2^+ + e \rightarrow N^* + N^{**}$	$(R3)$

Although NO is a minor constituent, NO^+ is a major constituent of E and F1 regions. This is so because NO^+ is an end product of the important reaction T1$\rightarrow O^+ + N_2 \rightarrow NO^+ + N$.

I.3.3 Morphology Mixing processes predominant at lower levels, disappear at E-region, starting to predominate diffusive separation.

The understanding of the way free electrons distribute in the E-region is important for ionosphere physics research. For radiopropagation, electrons morphology is more important than that of the ions. The former affect the communications, the latter act in producing and/or destroying sources.

The critical frequency of the E-layer, foE is controlled by the solar zenith angle, as can be seen in Figs. 6 and 7 (Equinox and Solstice) [6].

Superimposed on normal E-layer, and sometimes masking it in ionograms, one or more patches of denser ionization exist at heights of 100 to 120 km. They are called "sporadic-E" layers because they do not show a "regular" behaviour.

IGY definitions for sporadic-E reflections are:

(1) random time of occurrence;

(2) partial transparency (echoes also obtained from higher layers);

(3) variation of penetration frequency with transmitter power;

(4) virtual height independent of frequency.

It is very difficult to infer the existence of localized ionization sources as to produce E_s, because the sporadic's lifetime is much greater (some hours) than ions lifetime (few minutes). A good approach to the adequate model is the wind-shear theory (redistribution of ionization) [7]. It suggests that horizontal winds in the E-region neutral air support large vertical velocity gradients. As a consequence shear efforts may appear. These shears can redistribute the E-region ionization, Fig. 8 [8] illustrates a possible process.

The wind drags the positive ions. They experience a $\vec{V} \times \vec{B}$ force, being driven at an angle to the wind velocity, so they accumulate within the shear. The electrons, quite unaffected by neutral wind, move along magnetic field lines so as to neutralize the space charge set up by the ion motion.

This theory meets serious quantitative difficulties, which could be overcome by supposing that the E_s are composed of long-lived ions, such as metallic ions. Experimental evidence shows the existence of Ca, Mg and Fe, specially Mg with about a 70% of abundance. The origin is attributed to meteorites.

I.4 F–Region

The F-region corresponds to the densest layer of the ionosphere with atomic O^+ ions (10^{11} to 10^{12} M^{-3}) as the dominant component. An additional subdivision may be found in F-region: the F1-region, transition between molecular and atomic ions, and the F2 region, with the peak of O^+ ions.

The F-region starts on the top of E-region, at about 140 km, with an undefined upper limit. The maximum electron concentration occurs from 250 to 500 km. Neutral gas constitutes the main part of the atmosphere at these heights with a composition markedly different from that at lower regions. In the lower F-region O and N_2, with predominance of N_2, are the principal constituents.

Because the F-region is responsible for HF communications, it is the most

studied of the ionospheric layers.

I.4.1 F1-Layer It exhibits a marked solar control. It appears at dawn, reaches a maximum near midday, and disappears at dusk. It only shows small perturbations with respect to an α-Chapman layer. It is more pronounced during summer, at minimum solar activity. At midday and near the equator, F1 reaches a peak at about 160 km, with density of about $2.5 \times 10^{11} m^{-3}$ for equinoxes and solar minimum, and about $10^{12} m^{-3}$ for solar maximum.

The critical frequency, foF1, if it corresponds to an α-Chapman layer, should vary with the solar zenith angle, daily and seasonally as

$$f_0 \alpha (\cos \chi)^{1/n}$$

with $n = 4$. However, n shows a seasonal variation, which seems to depend on latitude.

Figs. 9 and 10 [9] show the foF1 maps vs. latitude and local time, for June 1954 (solar minimum) and June 1958 (solar maximum). For solar minimum there is symmetry, which does not appear for solar maximum. Then, foF1 would be closer to a Chapman layer only during solar minimum.

The main source of ionization of F1 region is the Lyman continuum and the region of 20-35 nm. The predominant ions are NO^+ and O_2^+ in lower F1. O^+ becomes progressively more important, being the major ionized component above 170–200 km.

I.4.2 F2-Region It has a very complex phenomenology, because it is strongly affected by ionisation transport under the action of electromagnetic forces, diffusion and temperature variations. The principal source for ionization of the F2-region is the same as for F1, with the addition of the 45–65 nm region. The F2 ionization peak is formed because of the decreasing rate of electron loss process with increasing altitude.

Negative ions are practically absent, consequently, dissociative recombination for electrons and positive molecular ions is the unique important process $X^+ + YZ \rightarrow XY^+ + Z$; $XY^+ + e \rightarrow X^* + Y^*$. A great proportion of the neutral atmosphere is atomic, with production of atomic ions by photoionization.

Figs. 4 and 5 show that during daylight ions $30^+(NO^+)$ and $32^+(O_2^+)$ are predominant below about 165 km, $16^+(O^+)$ becoming dominant above this

altitude. During the night the transition occurs around 220 km. Since neutral O_2 is a minor constituent, a greater part of O_2^+ should be produced by transference reactions, which is true for NO^+.

At some level above F2 peak, O^+ gives way to the protonosphere dominated by H^+. The boundary is strongly influenced by a charge exchange reaction

$$H^+ + O \rightleftharpoons H + O^+$$

I.4.3 α-and β-Chapman layers

$$\begin{array}{lllll} & & & R1 & \\ & & O_2^+ & \longrightarrow & O, O \\ & Q1 \quad T_2 \nearrow & & & \\ O \longrightarrow & O^+ & & & \\ & T_1 \searrow & & R2 & \\ & & NO^+ & \longrightarrow & N, O \\ & T_3 \quad \uparrow & & & \\ & Q_2 & & R3 & \\ N_2 & \longrightarrow & N_2^+ & \longrightarrow & N, N \end{array}$$

Operating with continuity equations suggested above for F-region, writing separate equations for electron concentration, N, for atomic ions, N_A^+ and for molecular ions, N_M^+, considering charge neutrality ($N = N_A^+ + N_M^+$), and neglecting the direct production of molecular ions by photoionisation, the following expression can be obtained.

$$\frac{1}{q} = \frac{1}{\beta N} + \frac{1}{\alpha N^2} \tag{4}$$

where α= dissociative recombination coefficient

$$\beta = \gamma \cdot n[M]$$

$\gamma =$ transfer or interchange coefficient

$n[M] =$ molecular gas concentration

Limiting cases:

$$\begin{aligned} q &= \alpha N^2 \text{ if } \beta >> \alpha N, \text{ so } N_M^+ >> N_A^+ \\ q &= \beta N \text{ if } \beta << \alpha N, \text{ so } N_M^+ << N_A^+ \end{aligned} \tag{5}$$

From the positive root of Eq.(4)

$$N = (q/2\beta)(1 + (1 + 4\beta^2/\alpha q)^{1/2})$$

the following expressions can be obtained

$$\begin{aligned} N = N_\alpha &= (q/\alpha)^{1/2} \quad \text{if} \quad 4\beta^2 >> \alpha q \\ N \simeq N_\beta &= q/\beta \quad \text{if} \quad 4\beta^2 << \alpha q \end{aligned} \tag{6}$$

which are equivalent to (5). Replacing (2) in (6)

$$q = q_{mo} \exp(1 - y - \sec\chi e^{-y}) \tag{2}$$

$$N_\alpha = (q_{mo}/\alpha)^{1/2} \exp \frac{1}{2}(1 - y - \sec\chi e^{-y})$$

$$N_\beta = (q_{mo}/\beta) \exp(1 - y - \sec\chi e^{-y})$$

N_α is called an α-Chapman layer, and N_β a β-Chapman layer. N_β applies at greater heights. However, in the actual F-region the Chapman simple theory does not hold well.

I.4.4 Morphology The morphology of F2 is much more complex than that of F1, Fig. 11 [9] shows foF2 global contours for equinoxes and solstices, for maximum solar activity (1947) and minimum solar activity (1943-44).

Certain features of great scale, consequences of the F2 ionization solar control, are common to all diagrams. The critical frequency increases after sunrise, this increment being more rapid at low latitudes. A maximum is reached early in the afternoon, followed by a rapid decrease after sunset. The critical frequencies are greater near the equator.

The differences between the F2 layer global behaviour and that of a hypothetic Chapman layer, called "anomalies", are as follows:

(i) The diurnal variation may be asymmetrical about noon, with rapid changes at sunrise and slow changes at sunset. The daily maximum can occur before or after noon in summer, and near noon in winter.

(ii) The diurnal variation does not repeat itself from day to day. This makes prediction more difficult and because of its importance in radio communications the F2 layer is the one for which accurate predictions are valuable.

(iii) The seasonal variation is anomalous in several ways. Values for foF2 at noon are said to be greater in winter than in summer - the winter anomaly - although some recent results are demonstrating that this effect manifests itself more at the north than at the south hemisphere.

(iv) A substantial F2 region is maintained at night.

(v) The Appleton or equatorial anomaly.

Briefly, three processes can be pointed out which probably account for most of the phenomena: (1) chemical changes, (2) diurnal heating and cooling, and (3) winds and electric fields.

The equilibrium electron density depends on the ratio O/N_2 and also on O/O_2. Seasonal anomalies could be due to seasonal changes in relative concentrations of atomic and molecular species, processes attributed to the global circulation of the atmosphere.

The maintenance of the F-region during the night might be explained by two processes, (a) the fact that plasma temperature exceeds that of neutral air. Then, the plasma moves up to greater altitudes, where it is stored due to the smaller rate of recombination. When the plasma cools at night, it moves down again helping to maintain the F-region; (b) the replenishment from the plasmasphere. The third major source of F-region anomalies is the neutral air wind at heights around 300 km.

The equatorial F-region presents an interesting anomaly, called "Appleton or equatorial anomaly". Based on a simple theory, the electron density should be a maximum over the equator at the equinox. Actually the density falls to a minimum over the magnetic equator and passes through maxima at about +30° and -30° magnetic dip. The anomaly exists during most of the day, being most pronounced around sunset. Generally, it disappears after midnight.

The phenomenon could be explained by the "fountain effect" process. Plasma is lifted through $\vec{E} \times \vec{B}$ electromagnetic drift. An electric field to the east and a horizontal magnetic field produce a plasma flow in the vertical, meeting some field lines down which it may diffuse under gravity. Figs. 12 and 13 show the phenomenon [10),11)]

A parameter responsible for several effects on earth-space propagation, defined as the total number of free electrons in a column of unit cross section along the path from a satellite to a ground station – Total Electron Content (TEC) – exhibits almost similar behaviour than N_mF2 (maximum F2 electron concentration) [12),13)].

In addition to great scale regular motions of ionization, the F-region

presents turbulent or irregular movements, called "spread-F" because of their appearance on ionograms, which show traces rather diffused. There are two main types of spread-F, spread on frequency and spread on height (range spread), the former attributed to strong scattering irregularities [14),15)].

The frequency spread is classic at middle and high latitudes, being the range spread typical of equatorial zones. Irregularities were measured over lengths from hundreds of km to tens of cm.

Range spreading is often associated with "bubbles", biteouts of ion concentration in the night time equatorial spread-F region. Highly structured upward velocity within the depleted regions ($\sim$ 100 m/s) justifies the name bubbles. Experiments confirm the existence of these vertical rising bubbles [16),17),18)].

The effects of irregularities on radiopropagation are most important on a path that crosses the equator. Efforts have been concentrated recently on the effects of irregularities on transionospheric propagation, where the problem of "scintillation" is encountered. This scintillation is produced in a radiowave when it traverses ionospheric irregularities, experiencing fading, phase deviations, and angle or arrival variations.

I.5 Transport in the Ionosphere

Electrons and ions are considered as a gas, a plasma, which is a minor constituent of the atmosphere. Like other gases, it is subject to gravity and collisional forces, and it is also acted upon by electric and magnetic forces.

The most important transport processes are:

(a) motion of ions and electrons by electric fields, these movements depending on magnetic field and collision frequencies;

(b) motion of charged particles by neutral winds. In the E-region these winds are mainly associated with tidal motions and in F-region they are driven by daily heating and cooling of the atmosphere;

(c) Thermal expansion and contraction of the atmosphere by daily temperature changes;

(d) Plasma ambipolar diffusion under the action of gravity and gradients in partial pressure, and due to electrical forces that tend to keep together

both types of components, with both kinds of particles moving at the same speed. Diffusion is more rapid in the upper than in the lower F-region.

The mathematics might be very complex involving continuity, motion and energy equations, but many times special physical conditions in the region of interest can help to reduce the set of equations to a more easy handling form.

II. THE MAGNETOSPHERE

II.1 Morphology

In the case of our planet, the magnetosphere can be defined as the space region surrounding the Earth in which the geomagnetic field controls the behaviour of the plasma it contains. It extends from the ionosphere up to 10 earth radii towards the sun, and to more than 1000 earth radii in the opposite direction (magnetosphere tail). This structure is created by the action of the solar wind flux which compresses the daylight side of geomagnetic field lines and combes them on the nocturnal side (see Fig.14) [10)].

The separation surface between solar wind and magnetosphere is called magnetopause. Since the solar wind is supersonic, a bow shock in front of the magnetopause is formed. Through this bow shock the solar wind plasma is damped and compressed. The region between the bow shock and the magnetopause is called magnetosheath, and it is filled by subsonic plasma and turbulent magnetic field.

Other typical regions of the magnetosphere interior are: the entry layer; located behind the foremagnetopause, is a region of direct capture of solar plasma. Some of the entrance particles eventually precipitate into the atmosphere along the geomagnetic field lines at high latitudes, but most of them are magnetically reflected, escaping along the extended magnetic field tail. These electrons and ions of solar wind origin, form the plasma mantle. Other fraction of solar wind particles drift longitudinally around the earth, refilling the plasmasheet region at the magnetic tail near the equatorial plane.

High energy ions and electrons, drifting in the geomagnetic field, form an equatorial ring current. During a geomagnetic storm the ring current flux of particles gets intensified. The general characteristics of the hot plasma that generate the auroral processes are not proper of the high latitude ionosphere, but they

correspond to the plasmasheet. Particles of this region can deeply "dive" along high latitude geomagnetic field lines into the atmosphere, collisioning with atmosphere atoms and exciting them. They disexcite with emission of auroral light. Besides the hot particles of the plasmasheet and ring current, the magnetosphere contains electrons and protons even more energetic. They form the trapped or Van Allen radiation belts. Deeper in the interior of the magnetosphere, at 4 or 5 earth radii, exists the plasmasphere, limited by a surface approximately aligned with the field and called plasmapause. The plasmasphere is a large reservoir of low energy plasma corrotating with the earth.

II.2 Generation and Dynamics

The boundary of the geomagnetic cavity is a surface such that at every point the pressure of the solar wind just outside the boundary is balanced by the pressure of the geomagnetic field just inside. The field into the cavity is distorted, with characteristics such as:

(a) the field lines from low latitudes still form closed loops between southern and northern hemispheres,

(b) Lines emerging from the poles, and merged with interplanetary magnetic field (IMF), are swept back away from the sun (open lines),

(c) there are two high latitude field lines that intersect the magnetopause forming neutral points (field intensity vanishes) when the boundary is reached.

The magnetotail is perhaps the most remarkable feature of the magnetosphere and it is the source of phenomena that are visible from the ground. There, the magnetic field tends to lie parallel to the solar wind downstream from the earth. Beyond about 10 earth radii (R_E), the field is deformed into a tail, whose boundary with the solar wind is roughly cylindrical, the field pointing approximately towards the earth in the northern half and away in the southern half.

Two mechanisms for transferring energy to the magnetosphere have been developed: Axford-Hines viscous interactions and Dungey magnetic merging. Recent satellite observations suggest that both mechanisms are operative, but in more complex ways than envisaged by early proponents.

The Axford-Hines model postulates that the magnetosheath plasma exerts a viscous force on a layer of unspecified thickness inside the magnetopause. Magnetic field lines threading this layer are dragged in the antisolar direction and are stretched to great distances in the magnetotail. As elongated flux tubes move out of the viscous interaction layer they snap back to a more dipolar configuration. Plasma trapped on the elongated flux tubes is adiabatically heated as the flux tubes convect earthward and shrink in volume (Fig. 15) [20].

The Dungey model postulates that the solar wind-magnetosphere dynamic interaction proceeds by means of a magnetic merging process. This process, illustrated in Fig. 16, considers a magnetic field that at great distances above (below) the X-Y plane points in the +(−) X direction. In the presence of an electric field E_Y, magnetic field lines convect toward the X-Y plane. At the neutral line (X=0, Z=0), magnetic lines from the upper half space merge with field lines of the opposite polarity from the lower half space. To the left (right) of the neutral line, merged lines cross the X-Y plane with A+(−)Z component, and $\vec{E} \times \vec{B}$ convect away from the neutral line in the +(−) direction.

When considerations on convection processes are made it is necessary to bear in mind that at these levels the fields $\vec{B}$ and $\vec{E}$ and the plasma drift velocity $\vec{V}$ satisfy the "freezing-in" equations

$$\vec{E}' = O = \vec{E} + \vec{V} \times \vec{B}; \quad \vec{V}_\perp = (\vec{E} \times \vec{B})/B^2$$

in which $V_\perp$ is the component of motion normal to $\vec{B}$. Basically, the theorem states that the ionised matter and magnetic field move in such a way that

(i) a set of particles, if connected by a field line, remains so connected at all times,

(ii) any given tube of plasma bounded by a set of field lines always encloses the same magnetic flux.

Now, coming back to the magnetic merging problem, it may be said that for the process to be carried out there are several possible magnetic topologies.

The IMF, carried by the solar wind, does not practically play an obvious role in viscous interaction model. However, the magnetic merging model assigns important roles to the IMF, requiring three types of magnetic field lines (1) IMF lines with both "feet" in the interplanetary medium (2) closed field lines with both "feet" on the Earth, and (3) open field lines with one "foot" on Earth and the other in the solar wind. The merging idea is illustrated Fig.17, a time history of an individual field line.

Merging occurs at time 1. Times 2 through 5 show the various stages of antisunward motion of an open field line. At time 6, a portion of the field line has convected to the magnetic equatorial plane where it reconnects with an open field line from the conjugate ionosphere. Under the influence of the dawn to dusk electric field, the field line convects earthwards (time 7 through 9). Eventually, the connected field lines move to the dayside (time 10) where they are in a position to continue the merging–reconnection cycle.

The plasmasheet, which is a highly dynamical region that acts as a depository for auroral particles, using the merging process energy transfer energizes the particles that precipitating along geomagnetic field lines, generate auroras and the auroral electrojet at the auroral E-region, with magnetic substorm signatures at ground.

III. MAGNETOSPHERE–IONOSPHERE COUPLING

The ionosphere and magnetosphere are coupled in so many different ways that nearly every magnetospheric or ionospheric process has its origin or its effect in the other link of the chain. The only way to approach to a full understanding of the complex mechanisms in play is by doing a "systemic" study of the magnetosphere and ionosphere, that is, to view both as an entire system. However, to synthesize, only the highlights of processes linking both regions will be presented.

It must be kept in mind that static ionosphere and magnetosphere never exist. At most, we must talk of "dynamic quietness" of the system.

III.1 Quiet Conditions

Vasyliunas [21] has developed a theoretical model that illustrates the physical laws describing the magnetosphere-ionosphere coupling. Fig.18 is a reproduction of Vasyliunas' original diagram. Boxes indicate quantities to be calculated and the label on each line refers to the physical principle or equation that links the two physical quantities. External sources of particles, cross-magnetospheric potentials, neutral winds in the ionosphere, are some of the imposed boundary conditions. It is possible to enter at any point of the loops.

Greenwald [22] has considered as invalid one of the simplifying assumptions, that of equipotential magnetic field lines, which means the existence of

parallel electric fields. This fact is fundamental at the expansion onset of substorms.

Assuming that we have an initial idea about the distribution of magnetospheric electric fields and particles, we get

(a) first link; we calculate the motion and distribution of protons and electrons in the magnetosphere, and hence the total plasma pressure at any point.

(b) second link: from the plasma pressure gradients, we can calculate the components of the electric current perpendicular to the magnetic field.

(c) third link: by calculating the divergence of the perpendicular current and averaging over each flux tube, the magnetic field-aligned currents (FAC) flowing between the magnetosphere and ionospere can be obtained.

(d) fourth link: from the requirement that FAC be closed by perpendicular ohmic currents in the ionosphere, it can be obtained the configuration of the electric field in the ionosphere.

(e) Fifth and final link: the ionospheric electric field can be mapped into the magnetosphere, and the requirement that it agrees with the magnetospheric electric field assumed at the onset determines the field, and thus closes the system of equations. Except near discrete auroral arcs, the mapping may be done assuming that magnetic field lines are equipotentials.

FAC are concentrated in three principal areas which encircle the geomagnetic pole, the auroral oval. Fig. 19 [23] is a summary of those currents, for weakly disturbed conditions.

1. "region 1" consists of current sheets which approximately follow the auroral oval. The current flows into the ionosphere at dawn and out of it at dusk;

2. "region 2" adjoins the above on the equatorward side, with opposite polarities;

3. cusp currents are located poleward of region 1 in the cusp region and are also of opposed polarities.

The fourth link specified above, involves a latitudinal localized iono-

spheric current, the auroral electrojet.

Downward current flow near noon diverges into the ionosphere as the eastward electrojet. Downward current flow near noon and in the late morning sector diverges into the ionosphere as the westward electrojet.

The current configuration sketched above suffers strong modifications during substorm activity.

The discovery of energetic O^+ ions conducted to a reevaluation of the sources of plasma which populate the magnetosphere. Prior to these measurements, the prevailing idea was that the solar wind was the principal source of the hot plasma throughout the magnetosphere. The discovery of O^+ ions of obvious ionospheric origin opened up a broad range of possibiliites for plasma sources and energization mechanisms for low energy ionospheric ions of all species.

Ionospheric ions ($He^+, He^{++}, O^+, O^{++}$) have been observed in the plasmasphere, ring current, magnetotail plasmasheet and lobes.

Two important processes led to the now accepted idea of ionosphere-plasmasphere interchange during quiet conditions: the maintenance of the nocturnal F-region and the nighttime enhancements in TEC [24),25),26),27)].

III.2 Perturbed Conditions

In analogy with weather storms on Earth's surface, drastic perturbations of the geomagnetic field from normal behaviour have been called geomagnetic storms.

During a period of high geophysical activity, when high-latitude magnetometers show very strong variations (bays) from normal conditions, which can reach values over 1000 nT, magnetometers at middle or equatorial latitudes may show patterns like those indicated in Fig.20.

The classical magnetic storms consist of three phases:

(1) an increase of the magnetic field lasting a few hours (initial phase);

(2) a pronounced decrease in the H component, reaching a maximum in about one day (main phase), and;

(3) a slow recovery phase in H, reaching normal values over several days.

The initial phase is caused by the compression of the magnetosphere by an intensified solar plasma, often related to solar flares. The second or main phase could be explained by an electric current encircling the earth at a few earth radii, the ring current. Space observations place it at 4-6 earth radii. It is produced by the drift of protons to the west and electrons to the east.

The magnetic storm has associated perturbations of the neutral and ionized upper atmosphere, with profound influence on its global morphology, constituting an important link in the complex chain of solar-terrestrial relations, since their energy is ultimately supplied by solar wind. This subject is also of practical interest since transionospheric and ionospheric radio communications and satellite ephemeris predictions may be severely degraded during these events.

One of the most studied parameters is N_mF2. Studies established that at midlatitudes N_mF2 may be enhanced (positive ionospheric storm effects) and/or depressed (negative ionospheric storm effects) during a magnetic storm (see f.i. [28),29)]).

Measurements of TEC show variations very similar to those observed in N_mF2, which means that N_mF2 changes do reflect the behaviour of the entire F2 layer and are not simply due to a distortion of the ionization height profile.

The positive phase could be attributed to:

(a) increment in production, originated by an increase in solar's ionizing radiation; in auroral sones could be due to precipitation of particles from the magnetosphere.

(b) downward plasma flux from the plasmasphere, produced by its compression. This flux would propagate along magnetic field lines (a "tooth paste" tube effect).

(c) $\vec{E} \times \vec{B}$ drift of ionized particles from the plasmasphere, due to the appearance of an adequate component of a great scale induced electric field.

(d) lifting of plasma produced at low levels up to heights where electron's loss rate is smaller. This process may be produced by winds and/or electric fields.

The negative phase could be attributed to:

(a) increment in the electron's loss rate, due to the increment of the loss

reaction chemical coefficients caused by an increase in ion's temperature.

(b) changes in the neutral composition.

No overview of magnetospheric-ionospheric disturbances would be satisfactory without comments on high-latitude substorms. It is during substorms that the dynamic coupling between both regions is most striking. The term substorm actually embraces a chain of very striking events: the magnetospheric substorm, the auroral substorm and the ionospheric substorm.

The aurora is the most readily observed consequence of the dynamic behaviour of the magnetosphere.

Substorm effects can be only understood in the context of the magnetosphere as a whole. The major points of agreement between various schools of thought are:

1. During extended periods of northward IMF the magnetosphere approaches to a ground state (not excited state, in analogy to the nucleus).

2. As the IMF turns southward, magnetospheric convection increases. This effect can exist for some time prior to substorm onset.

3. Substorm onset is signaled by an explosive increase in luminosity of the equatorward arc and an intensification of the auroral electrojet.

4. The expansion phase occurs from onset to the time when the midnight sector arcs have undergone their most poleward excursions.

5. The recovery phase coincides with the period in which the midnight sector arcs retreat equatorward.

The different schools met in August 1978 to specify substorm signatures and to get some agreement on causes and effects of such a phenomenon [30]. Briefly, the observations can be pieced together as follows.

1. At a southward turning of the IMF, magnetic flux is transferred from the day to the night side of the magnetosphere. This process proceeds for less than one hour in which potential energy, in the form of stored magnetic flux, builds up in the tail. During this period the neutral sheet and current moves earthward to $\sim 10R_E$ leading to a tail-like field geometry at $\sim 7R_E$.

2. At substorm onset, the neutral sheet current near the inner edge

of the boundary plasmasheet is diverted via FAC through the ionosphere. This leads to a collapse of the inner portion of the tail. In the ionosphere, part of the energy release in the tail collapse, appears as an explosive brightening of the most equatorward arc. As the inner-tail field lines snap back to dipolar, plasmasheet electrons are rapidly accelerated by electric fields and injected to the vicinity of geostationary distance. The process continues while B_z remains southward.

3. When IMF turns northward the rate of flux transfer decreases abruptly. If the IMF maintains a northward component for considerable time, the energy stored in the tail is slowly dissipated and the magnetosphere relaxes toward a ground state.

A new idea, developed in this decade, predicts the formation and expulsion of plasmoids at the magnetotail [31],[32],[33].

At the instant of an auroral onset, a new magnetic neutral line, called substorm neutral line, forms spontaneously in the plasmasheet about 15 R_E downstream from the earth (see Fig.21) [34]. This neutral line causes the disruption of the electric current that normally crosses the plasmasheet earthward of the line. As a result this part is suddenly reduced, so the magnetic field lines in the region become less stretched and contract toward the Earth, becoming more dipolar in shape. Meanwhile, the formation of a plasmoid has begun. The stretched field lines at the new neutral line start to reconnect, forming shortened closed field lines on the earthward side and closed loops on the tailward side of the neutral line. The latter spans the distance from the substorm neutral line to the presubstorm distant neutral line. The expulsion of plasma from the reconnection region carries the loops tailward and the shortened field lines earthward at speeds of several hundred km/sec. When the reconnections are complete, a set of nested (plasmoids) closed loops is free of the Earth. Its length is from 70 to 80 R_E; its width from 20 to 25 R_E. After the plasmoid forms, the surrounding open lines in the lobes reconnect to form a sheath of interplanetary field lines, which act as a slingshot propelling the plasmoid tailward at speeds of 500 to 1000 km/s.

IV. OTHER MAGNETOSPHERES PRESENT KNOWLEDGE (A SUMMARY)

As was specified, a magnetosphere arises from the interaction of a continuously streaming collisionless plasma with a magnetized body. Presently known magnetospheres scale from a few thousand kilometers in transverse dimension

(Mercury) to over ten million light years (radiogalaxy NGC 1625) [35].

Mariner 10 established that Mercury has an intrinsic magnetic field; the Pioneer Venus Orbiter has established that Venus has no significant intrinsic field. The existence of a martian magnetic field is controversial. No unambiguous signature of the field has been reported. The outer planets Jupiter, Saturn and Uranus are characterized by a now known strong intrinsic magnetic field. This section will give only an overview of Venus (no significant intrinsic magnetic field) and Jupiter's (strong intrinsic magnetic field) magnetospheres

IV.1 The Venus Magnetosphere

Unlike the Earth, Jupiter, Saturn, Uranus and Mercury, neither Mars nor Venus have a significant intrinsic magnetic field. However, each one possesses an envelope of well developed ionized gas (ionosphere). That is the reason why the ionized cavities surrounding Mars and Venus are called pseudo-magnetospheres.

The solar wind, during the interaction with Venus ionosphere, builds a bow shock detached from the planet, but much closer to it than in the case of the Earth. This difference arises from the fact that the obstacle that creates the bow shock is not the intrinsic magnetic field of Venus, but the small magnetic field produced by the currents induced in the ionosphere by the solar wind flux. The interplanetary magnetic field, which moves with the solar wind's plasma, cannot penetrate the electrically conducting ionosphere and accumulates in front of the planet, forming a magnetic barrier to the solar wind.

Fig. 22 [36] shows altitude profiles of observed ionospheric magnetic field (not intrinsic) and electron density for two orbits of the Pioneer Venus Orbiter (PVO). The neat upper order, with a fast decrease in density, is called the ionopause, it is a typical feature of the Venus ionosphere.

The measurements of Venera 9 and 10 revealed that Venus has an Earth-like extended plasma-magnetic tail which has a diameter slightly greater than the planet's diameter (Fig. 23) [37]. Immediately behind the nocturnal ionosphere exist a cone-shaped region (C), the corpuscular umbra. There the flux of ions is weaker than downstream of the transition region (A). Region (E) is the plasma sheet inside which the neutral layer is located. It separates oppositely directed field lines.

IV.2 The Jupiter Magnetosphere

In no way is Jupiter an ordinary planet. It is the greatest one of the solar system with a mass over the double of the mass of all other planets together. Jupiter radiates more caloric energy than that received from the Sun. So, judging from the energetic activity, Jupiter may be considered rather a weak star than a planet. More than three decades ago it was discovered that Jupiter is a strong emitter of radio noise, and the most brilliant radio source in the sky. This emission originates in the internal part of an active and so big magnetosphere that, if it could be seen, it would appear from the Earth as the greatest object in the sky, and with variations from two to more than four times the lunar or solar diameter (relative angular sizes). Sixteen natural satellites are orbiting around Jupiter, being IO possibly the most volcanic body known in the solar system.

In the region inside 20 Jupiter's radli (R_J), the magnetic field is dipole-like, except near the planet's surface where the structure of the field is more complex involving magnetic anomalies. Farther of 20 R_J the magnetic field is elongated (Fig. 24). The encounter of the Pioneer 10 with Jupiter revealed that such a distended configuration exists even on the diurnal side, a fact that does not manifest itself in the terrestrial magnetosphere. Such a configuration looks qualitatively like the nocturnal Earth's magnetospheric tail.

Energetic particle measurements in the Jovian magnetosphere showed time variations in phase with the 10 hours planetary rotation period [38],[39],[40]. These observations are interpreted in terms of a physics model in which the Jovian magnetosphere is inflated by ionospheric plasma, which is accelerated by the corrotation centrifugal force. This process causes a disklike magnetic field configuration on the diurnal side and a planetary wind of leak of plasma on the nocturnal side which eventually evolves in a magnetic tail. Even before the arrival of the first probe to Jupiter, Gledhill [41] predicted the existence of such a disk. That is why the disk is called the Gledhill disk.

Some of the questions that came forth were the following: which is the energy source that handles the wide variety of Jovian's magnetospheric phenomena? Where do the plasma of the magnetodisk and of other places of the magnetosphere come from? It appears that the energy is extracted from the rotational energy of Jupiter itself; that is, its fast turn is being imperceptibly damped by the interaction with its own magnetosphere. Even more remarkable, the natural satellite IO is the primary source of the plasma that populates the magnetosphere and the

magnetodisk. Consequently, it appears that in Jupiter, unlike the Earth, the solar wind does not provide neither plasma nor energy. It becomes more reasonable to talk about the magnetospheric system Jupiter/IO rather than the magnetosphere of Jupiter.

The origin and distribution of plasma into the system is rather simple conceptually. Because of its volcanoes, IO is covered with condensed volcanic material, mainly frozen SO_2. Part of this material is expelled from IO, because of an intense bombardment by particles, with enough velocity as to escape from IO. This material is further ionized by additional bombardment of particles, forming a plasma torus near the orbit of IO, which is big and relatively massive in comparison with the Earth's magnetospherical plasma (1 million tons of SO_2 against 10 tons of material for Earth). This IO's plasma is transported and accelerated through the Jupiter's magnetosphere, so creating the most extensive and most energetic radiation belt of the solar system.

REFERENCES

1) F.J. Rich, "*Ionospheric physics*" in *Handbook of Geophysics and the Space Environment* (Chapter 9, Sec. 9.1), Ed. A.S. Jursa (Air Force Geophysics Laboratory, USAF, 1985).

2a) S. Chapman, "*The absorption and dissociative or ionizing effect of monochromatic radiation in an atmosphere on a rotating earth*", Proc. Phys. Soc. (London) **43**, 26 (1931).

2b) S. Chapman, "*The absorption and dissociative or ionizing effect of monochromatic radiation in an atmosphere on a rotating earth II. Grazing incidence*", Proc. Phys. Soc. (London) **43**, 483 (1931).

3) H. Rishbeth and O.K. Garriott, *Introduction to Ionospheric Physics*, (Academic Press, 1969) p. 93.

4) L.J. Heroux and H.E. Hinterwegger, "*Solar ultraviolet irradiance*", in *Handbook of Geophysics and the Space Environment* (Chapter 2) Ed. A.S. Jursa (Air Force Geophysics Laboratory, USAF, 1985).

5) J.C. Holmes, C.Y. Johnson and J.M. Young, "*Ionospheric chemistry*", in *Space Research*, Vol V, p.756, Eds.King-Hele, Muller and Righini, North Holland Pub., 1965).

6) K. Davies, *Ionospheric Radiopropagation*, p.139 (Dover Publications, 1966).

7) J.D. Whitehead, "*The formation of the sporadic-E layer in the temperate zones*", J. Atmos. Terr. Phys. **20**, 49 (1961).

8) C.O. Hines, "*The formation of mid-latitude sporadic E layers*", J. Geophys. Res. **69**, 1018 (1964).

9) D.F. Martyn, "*The normal F region of the ionosphere*", Proc IRE N.Y. **47**, 147 (1959).

10) S.A. Croom, A.R. Robbins and J.O. Thomas, "*Two anomalies in the behaviour of the F2 layer of the ionosphere*", Nature **184**, 2003 (1959).

11) J.W. King, K.C. Reed, E.O. Olatunji and A.J. Legg, "*The behaviour of the topside ionosphere during storm conditions*", J. Atmos. Terr. Phys. **29**, 1355 (1967).

12) J.E. Titheridge, "*Continuous records of the total electron content of the ionosphere*", J. Atmos. Terr. Phys. **28**, 1135 (1966).

13) R.G. Ezquer and N. Ortiz de Adler, "*Electron content over Tucuman*", (accepted for publication at J. Geophys. Res. , 1988).

14) W. Calvert and R. Cohen, "*The interpretation and synthesis of certain spread - F configurations appearing on equatorial ionograms*", J. Geophys. Res. **66**, 3125 (1961).

15) R.G. Rastogi, "*Seasonal and solar cycle variations of equatorial spread - F in the american zone*", J. Atmos. Terr. Phys. **42** 593 (1980).

16) R.F. Woodman and C. La Hoz, "*Radar observations of F region equatorial irregularities*", J. Geophys. Res. **81**, 5447 (1976).

17) K.C. Yeh, H. Soicher and C.H. Liu, "*Observations of equatorial ionospheric bubbles by the radiopropagation method*", J. Geophys. Res. **84**, 6589 (1979).

18) A. Das Gupta, J. Aarons, J.A. Klobuchar, S. Basu and I. Bushby, "*Ionospheric electron content depletions associated with amplitude scintillations in the equatorial region*", Geophys. Res. Letters **9**, 147 (1982).

19) R.H. Eather, *Majestic Lights*, (American Geophysical Union, Washington, 1980).

20) W.J. Burke, D.A. Hardy and R.P. Vancour, "*Magnetospheric and high latitude ionospheric electrodynamics*", in *Handbook of Geophysics and the Space Environment* (Chapter 8), Ed. A.S. Jursa (Air Force Geophysics Laboratory, USAF, 1985).

21) V.M. Vasyliunas, "*Mathematical models of magnetospheric convection and its coupling to the ionosphere*", in *Particles and Fields in the Magnetosphere*, Ed. B.M. McCormac, p. 60, (D. Reidel, 1970).

22) R.A. Greenwald, "*Recent advances in magnetosphere-ionosphere coupling*", Rev. Geophys. Space Phys. **20**, 577 (1982).

23) T.A. Potemra, *Dynamical and Chemical Coupling*, Ed. Grandal and Holtet (D. Reidel, 1977) p. 337.

24) J.E. Titheridge, "*The maintenance of the night ionosphere*", J. Atmos. Terr. Phys. **30**, 1857 (1968).

25) N. Balan and P.B. Rao, "*Latitudinal variations of nighttime enhancements in total electron content*", J. Geophys. Res. **92**, 3436 (1987).

26) R.G. Ezquer, J.R. Manzano and N. Ortiz de Adler, "*Fuertes incrementos de contenido electronico total y densidad electronica, en condiciones geomagneticas diferentes*" (Strong increments of total electron content and electron density in different geomagnetic conditions), Revista de Geofisica (Espana) **40**, 43 (1984).

27) K. Davies, D.N. Anderson, A.K. Paul, W. Degenhardt, G.K. Hartmann and R. Leitinger, "*Nighttime increases in total electron content observed with the ATS 6 radio beacon*", J. Geophys. Res. **84**, 1536 (1979).

28) G.W. Prölss, "*Magnetic storm associated perturbations of the upper atmosphere: recent results obtained by satellite-borne gas analyzers*", Rev. Geophys. Space Phys. **18**, 183 (1980).

29) A. Martinez de Garat and J.R. Manzano, "*Comportamiento de la region F durante la tormenta geomagnetica del 1° de abril de 1976*" (F-region behaviour during the 1st of April 1976, geomagnetic storm) Revista Geofisica del IPGH, N. **16**, 93 (1982).

30) G. Rostoker, S.I. Akasofu, J. Foster, R.A. Greenwald, Y. Kamide, K. Kawasaky, A.T.Y. Lui, R.L. McPherron and C.T. Russell, "*Magnetospheric substorms. Definitions and signatures*", J. Geophys. Res. **85**, 1663 (1980).

31) E.W. Hones, D.N. Baker, S.J. Bame, W.C. Feldman, J.T. Gosling, D.J. McComas, R.D. Zwickl, J. Slavin, E.J. Smith and B.T. Tsurutani, "*Structure of the magnetotail at 220 R_E and its response to geomagnetic activity*", Geophys. Res. Letters **11**, 5 (1984).

32) T.G. Forbes and E.R. Priest, "*On reconnection and plasmoids in the geomagnetic tail*", J. Geophys. Res. **88**, 863 (1983).

33) M. Scholer, G. Gloeckler, D. Hovestadt, B. Klecker and F.M. Ipavich, "*Characteristics of plasmoid-like structures in the distant magnetotail*", J. Geophys. Res. **89**, 8872 (1984).

34) E.W. Hones Jr., "*The Earth's magnetotail*", Scientific American 254, 40 (1986).

35) J.G. Roederer, "*Global problems in magnetospheric plasma physics and prospects for their solution*", Space Sci. Rev. 21, 23 (1977).

36) R.C. Elphic, C.T. Russell and J.G. Luhmann, "*The Venus ionopause current sheet: thickness length scale and controlling factors*", J. Geophys. Res. 86, 11430 (1981).

37) K.I. Gringaus, "*A comparison of the magnetosphere of Mars, Venus and the Earth*", in *Advances in Space Research*, Cospar 1, 5 (1981).

38) J.A. Simpson, D. Hamilton, G. Lents, R.B. McKibben, A. Magro-Campero, M. Perkins, K.R. Pyle, A.J. Tuzzolino and J.J. O'Gallagher, "*Protons and electrons in Jupiter's magnetic field: results from the University of Chicago experiment on Pioneer 10*", Science 183, 306 (1974).

39) J.A. Van Allen, D.N. Baker, B.A. Randall, M.F. Thomsen, D.D. Sentman and H.R. Flindt, "*Energetic electrons in the magnetosphere of Jupiter*", Science 183, 309 (1974).

40) R.W. Fillius and C.E. McIlwain, "*Radiation belts of Jupiter*", Science 183, 314 (1974).

41) J.A. Gledhill, "*Magnetosphere of Jupiter*", Nature, 214, 155 (1967).

Figure Captions

Fig.1 Total ionization profile with ionospheric layers.

Fig.2 Normalized Chapman production function versus reduced height Z. Parameter: solar zenith angle χ (from Rishbeth and Garriott, 1969)[3].

Fig.3 The altitude at which the rate of absorption of solar UV radiation is at maximum. The principal atmospheric constituents that absorb the radiation in the different wavelength bands are indicated (from Heroux and Hinteregger, 1985) [4].

Figs.4 and 5 Daytime (above) and night time (below) positive ion composition (from Holmes et al., 1965)[5].

Figs.6 and 7 Maps of foE (from Davies, 1966) [6].

Fig.8 Idealized illustration of the wind–shear mechanism in the E region (from Hines, 1964) [8].

Figs.9 and 10 Maps of foF1 (from Davies, 1966) [6].

Fig.11 Maps of foF2 (median values) for (a) equinox, (b) June solstice for 1943-44 (minimum solar activity), (c) equinox, (d) June solstice for 1947 (maximum solar activity) (from Martyn, 1959) [9].

Fig.12 Variation of NmF2 and of electron concentration at fixed heights with magnetic dip, for noon on quiet days (September 1957) (from Croom et al., 1959) [10].

Fig.13 Latitude variation of electron concentration at fixed heights, from Alouette I topside sounder satellite (Singapore, September, 1963) (from King et al., 1967) [11].

Fig.14 A magnetosphereic model drawn ny Heikkila (from Eather, 1980) [19].

Fig.15 Equatorial projection of convection pattern in viscous interaction model (from Burke et al., 1985) [20].

Fig.16 Magnetic field geometry and electric field required for magnetic merging (from Burke et al., 1985) [20].

Fig.17 Snapshot of magnetic merging between southward IMF and the earth's

magnetosphere (from Burke et al., 1985) [20].

Fig.18 Logic diagram for a self-consistent calculation of magnetospheric convection (from Vasyliunas, 1970) [21].

Fig.19 The spatial distribution and flow directions of large-scale field aligned currents determined from data obtained during weakly disturbed conditions (from Potemra, 1977) [23].

Fig.20 Representative magnetic deviations during magnetic storms. (After M. Sugiura and S. Chapman, Abh. Akad. Wiss. Göttingen Math. Phys. Kl. Spec. Issue 4, 53, 1960).

Fig.21 Successive steps to the creation of a plasmoid during a magnetospheric substorm (from Hones, 1986) [34].

Fig.22 Altitude profiles of observed magnetic field (thin trace) and ionospheric electron number density (circles), measured at Venus (from Elphic et al., 1981) [36].

Fig.23 Schematic diagram of the Venus bowshock and magnetosphere (Venera -9 and -10 data) (from Gringauz, 1981) [37].

Fig.24 A cross-sectional view of Jupiter's magnetosphere in the plane in which the North magnetic pole is up and the Sun is to the left.

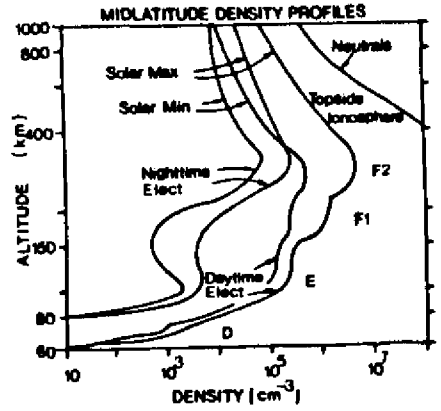

Fig. 1

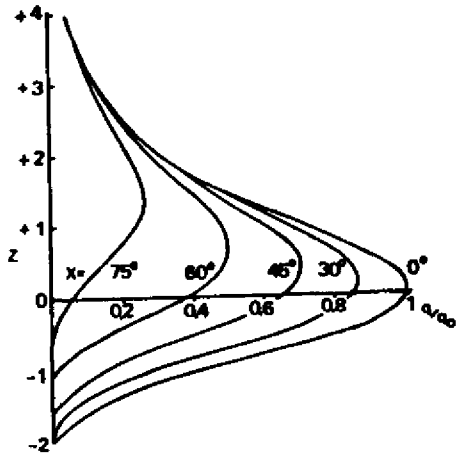

Fig. 2

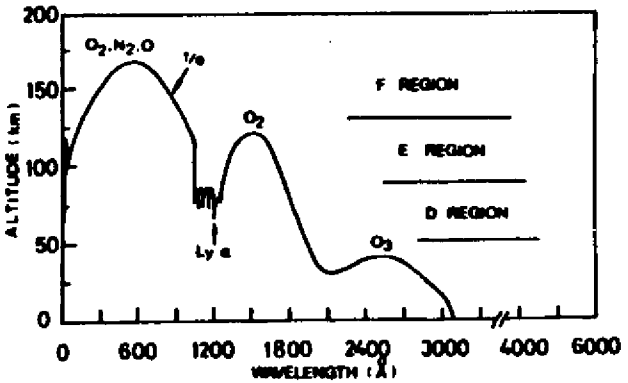

Fig. 3

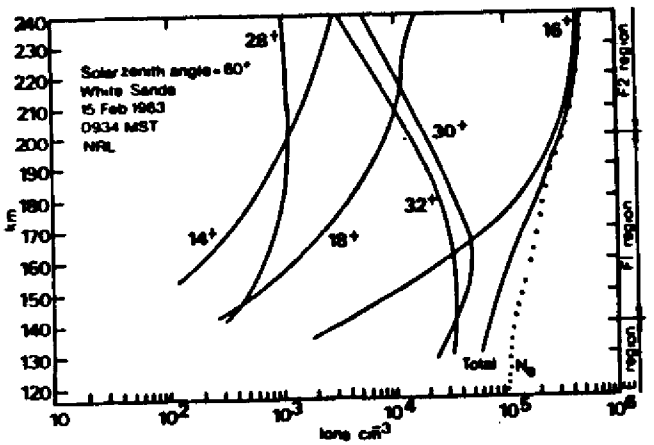

Fig. 4

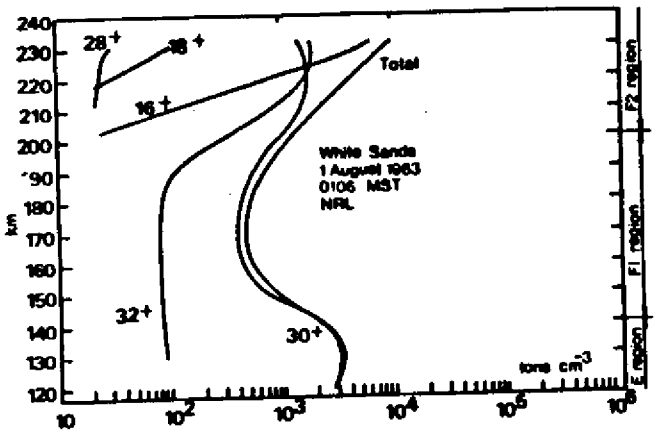

Fig. 5

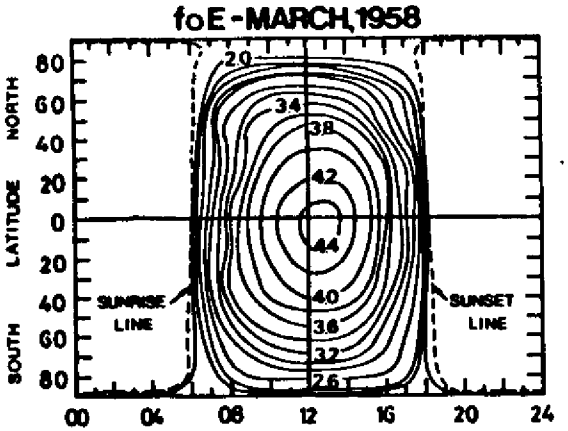

Fig. 6

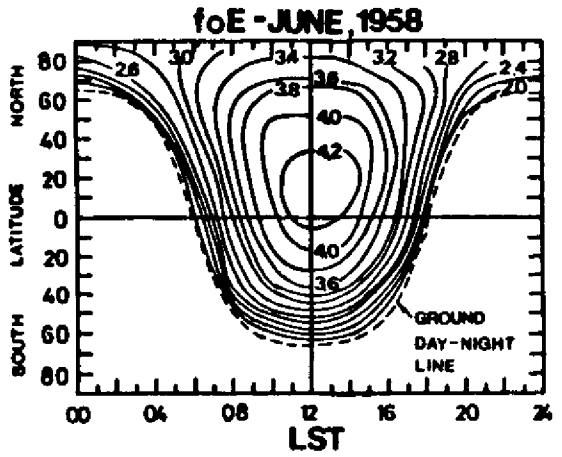

Fig. 7

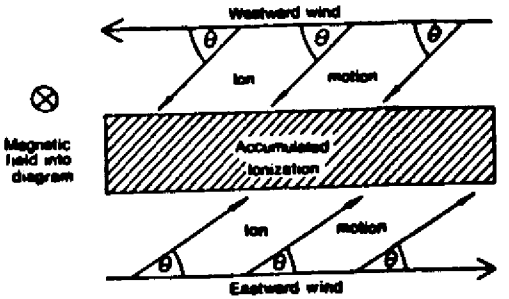

Fig. 8

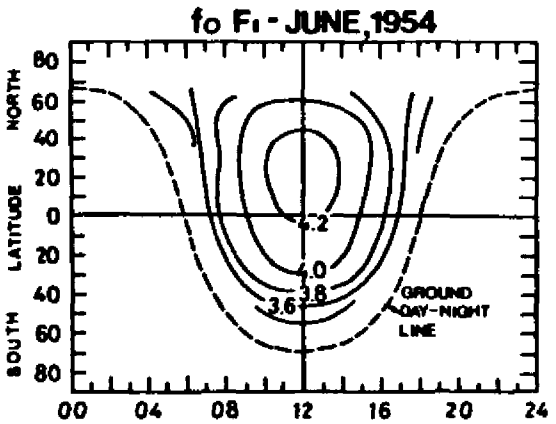

Fig. 9

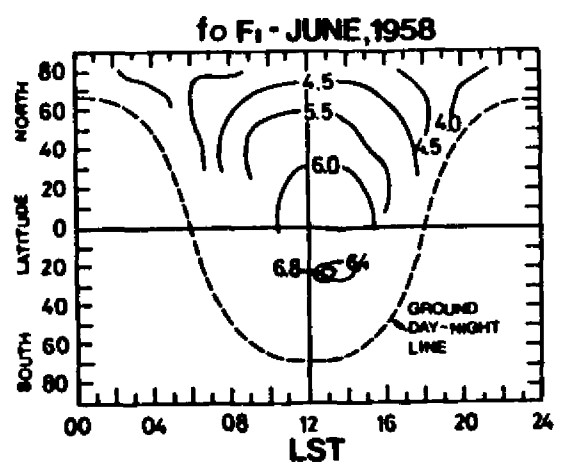

Fig. 10

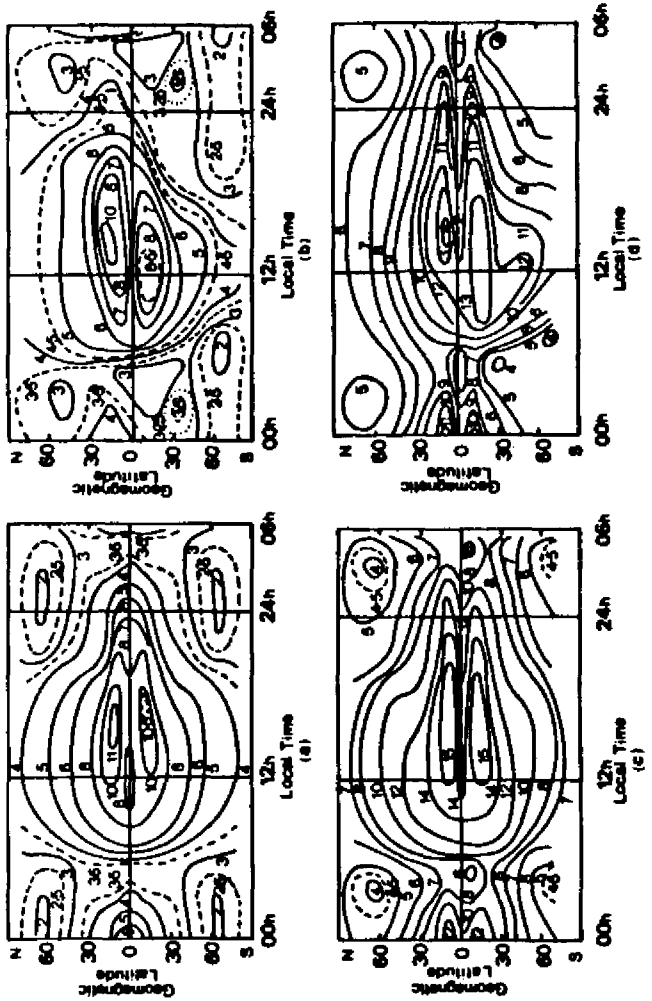

Fig. 11

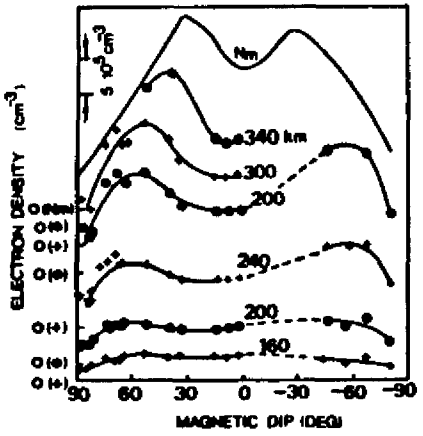

Fig. 12

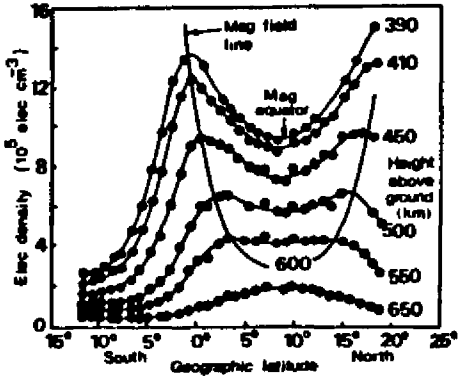

Fig. 13

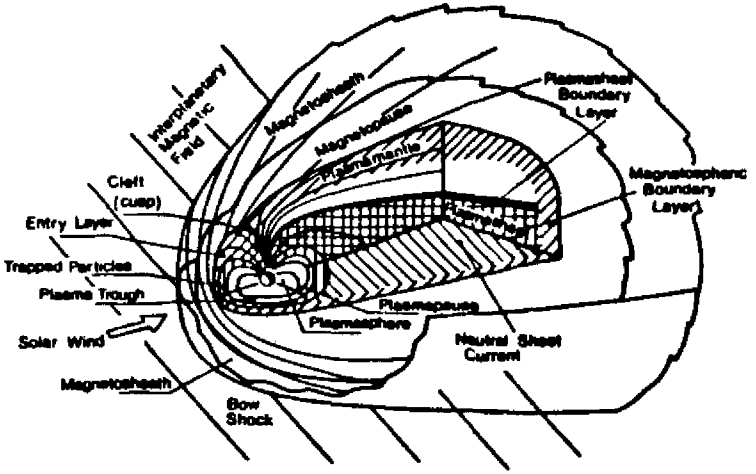

Fig. 14

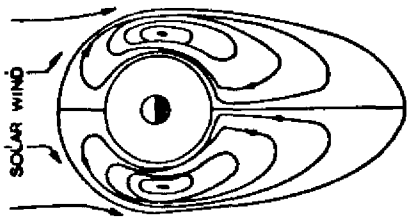

Fig. 15

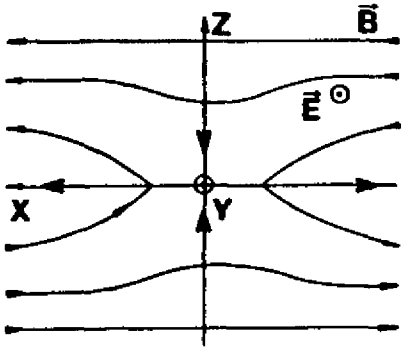

Fig. 16

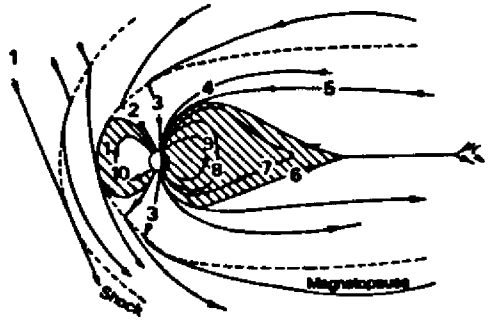

Fig. 17

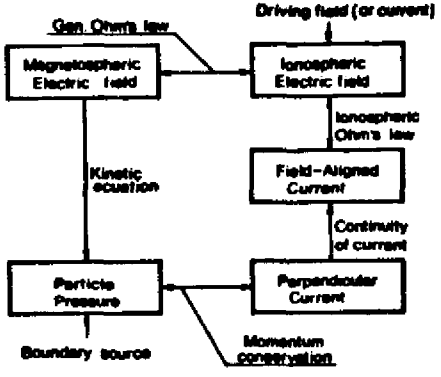

Fig. 18

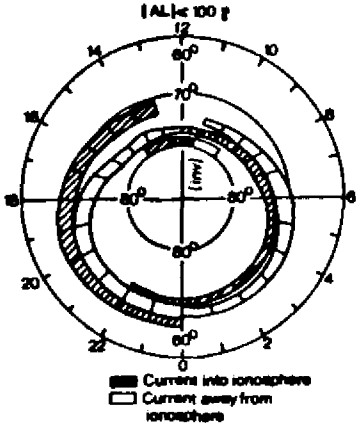

Fig. 19

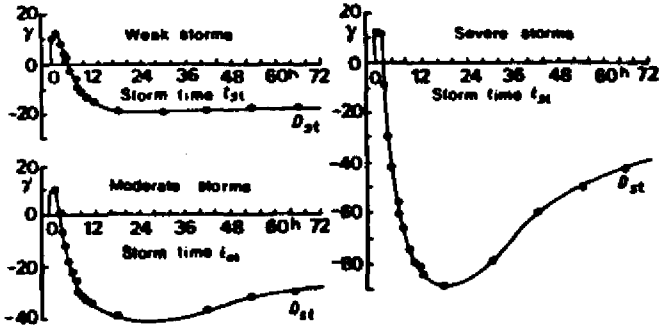

Fig. 20

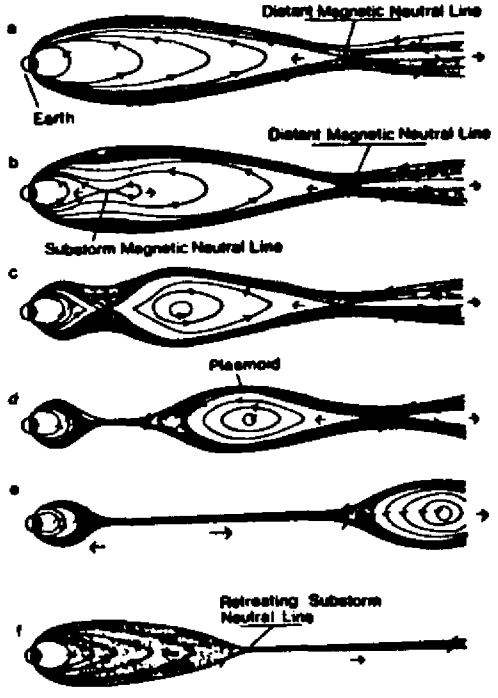

Fig. 21

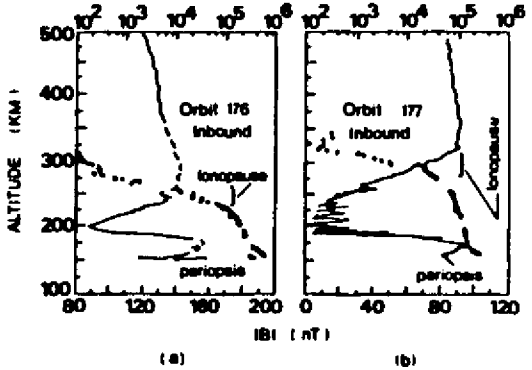

Fig. 22

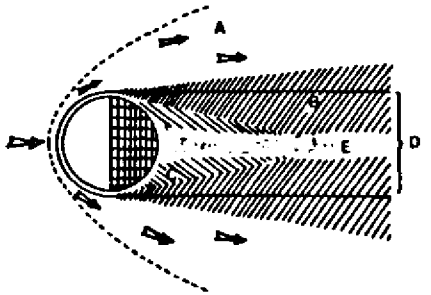

Fig. 23

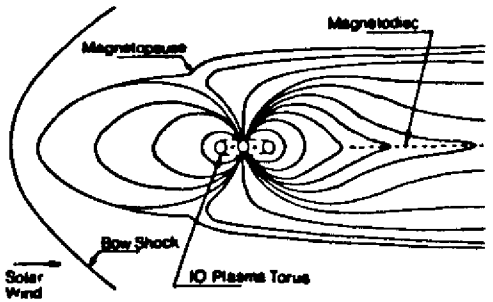

Fig. 24